

## Elastic electron scattering cross sections for Xe in the 1–100 eV impact energy region

D F Register<sup>†</sup>, L Vuskovic<sup>‡</sup> and S Trajmar

Jet Propulsion Laboratory, California Institute of Technology, Pasadena, California 91109, USA

Received 18 September 1985

**Abstract.** Relative differential elastic scattering cross sections for Xe have been measured in the 1–100 eV impact energy and 10–146° angular ranges. The data were subjected to phaseshift analysis, but the normalisation was achieved at each impact energy by utilising total electron scattering, ionisation and total excitation cross sections. Comparison is made with other recent experimental and theoretical results.

### 1. Introduction

Elastic electron scattering cross sections for Xe available up to 1978 have been summarised by Brandsen and McDowell (1978). Klewer *et al* (1980) reinvestigated the elastic angular distributions in the 2–300 eV impact energy ( $E_0$ ) region and made extensive comparisons with previous measurements and calculations. At impact energies of 100 eV and higher, they found good agreement in the shape of the available differential cross section (DCS) curves in the 50–100° angular range but not at the lower angles. At 50 eV the cross section curves were in serious disagreement while at the lower impact energies the angular distributions obtained by various investigators agreed quite well. At low impact energies Heindorf *et al* (1976), Weyhreter *et al* (1983) and very recently Holtkamp and Jost (1985) and Nishimura *et al* (1985a, b) reported differential cross section measurements. Recent theoretical results and comparisons with earlier calculations are given by Sin Fai Lam (1982a, b, semirelativistic method), Berg (1982,  $X_\alpha$  approximation), O'Connell and Lane (1983, non-adjustable model potential), McEachran and Stauffer (1984, optical potential model treating exchange exactly and including only the dipole part of the polarisation potential) and Kemper *et al* (1985, relativistic non-local two-channel theory).

Total electron scattering cross sections have been measured for Xe at impact energies ranging from 0.025 to 3000 eV. Recently, Hayashi (1983) summarised the available data and published recommended values for total scattering cross sections (as well as momentum transfer and total excitation cross sections) up to 10<sup>4</sup> eV. The most recent measurements in the impact energy range of interest to us here and a summary of previous data have been published by Nickel *et al* (1985). In addition, the results of Jost *et al* (1983) as quoted by Nickel *et al* have been revised (Jost *et al* 1985). At impact energies which are below the first inelastic threshold (8.32 eV), the total scatter-

<sup>†</sup> Present address: Phillips Petroleum Co, Bartlesville, OK 74003, USA.

<sup>‡</sup> Present address: Institute of Physics, PO Box 57, 11001 Beograd, Yugoslavia.

ing cross sections are equivalent to integral elastic cross sections and can serve to normalise relative DCS measurements or to cross check differential and integral cross section results obtained by other methods.

In recent years, electron scattering by Xe has been a challenging test of both experimental techniques and theoretical methods. The large dipole polarisability of this atom as well as the complicated dependence of the DCS on both energy and scattering angle provides formidable experimental problems. The non-*LS*-coupled nature of this system along with the complications of the many electron problem provide a stringent test for theoretical models. Recent measurements of the total electron scattering cross sections by Nickel *et al* (1985) coupled with the improved experimental and normalisation techniques provide an opportunity for improving the accuracy of elastic DCS for Xe below 100 eV impact energies.

In the present article we report elastic differential cross sections in the 1–100 eV impact energy and 10–146° angular ranges. These cross sections were obtained from relative angular distributions measured in a beam-beam experiment. At all impact energies the phaseshift analysis of Register *et al* (1980) was used to fit the distributions empirically and to extrapolate the relative cross sections to 0 and 180° scattering angles. Integration over all angles then yielded the integral elastic cross sections in arbitrary units which were normalised to cross sections obtained by a semi-empirical procedure from total electron scattering, ionisation and excitation cross sections.

## 2. Experimental procedures

### 2.1. Measurement of the elastic scattering signal

The apparatus used in the present measurements has been described earlier by Register *et al* (1980). The Xe beam was generated by a capillary array and further collimated by a skimmer. The skimmer chamber was differentially pumped by a high throughput pump. With this arrangement no effective path length correction was needed to transform the scattering intensities into relative differential cross sections (see Brinkmann and Trajmar 1981). The electron gun assembly utilised double hemispherical analysers and cylindrical electrostatic lenses to achieve high angular collimation in the electron beam. It was housed in a differentially pumped box and operated in the low-resolution mode ( $\text{FWHM} \approx 100$  meV). The atomic beam was crossed by the electron beam perpendicularly and the elastic scattering intensity was measured as a function of the scattering angles ( $\theta$ ) at fixed impact energies. The detector consisted of two angle-defining apertures, a retarding grid structure and a channeltron electron multiplier. This assembly could be rotated around the atomic beam axis from  $-30$  to  $+150^\circ$  with respect to the incoming electron beam. The retarding grid potential was adjusted to transmit only elastically scattered electrons and reject all inelastic electrons. With this arrangement the elastic scattering signal was obtained at the desired impact energy and scattering angle. The measured signal was corrected for the contribution from UV photons by biasing the retarding grids to reject all electrons and determining the signal associated with photons.

The impact energy scale was calibrated against the 19.37 eV resonance in He at  $90^\circ$  scattering angle. Changing from He to Xe could in principle affect the energy scale calibration. In the present case, because of the differentially pumped gun and very low background pressure ( $10^{-6}$  Torr) in the scattering chamber, this effect was

negligible. The true zero scattering angle was determined from the symmetry of the scattering signal in the  $-30$  to  $-10^\circ$  and  $+30$  to  $+10^\circ$  angular regions.

The 1 eV impact energy data were obtained with a spectrometer which used aperture optics and cylindrical energy analysers in both the gun and detector. This instrument was described by Hall *et al* (1973).

## 2.2. Phaseshift analysis

The  $\chi^2$  method used to obtain the real phaseshifts from the angular distribution curves has been described in detail by Register *et al* (1980). The technique described therein can be written in a more compact form following the derivation of Bevington (1969) which is briefly summarised here. The  $\chi^2$  for fitting the DCS may be written as

$$\chi^2 = \frac{1}{M-P-1} \sum_{s=1}^M \left( \frac{\sigma_x(s) - F(s)}{\sigma_x(s)} \right)^2 \quad (1)$$

where  $\sigma_x(s)$  is the  $s$ th data point with associated errors  $\delta\sigma_x(s)$ ,  $M$  is the number of data points and  $P$  is the number of phases varied.  $F(s)$  is the function used to fit the data ( $=N\sigma_F(s)$  in the earlier notation of Register). Defining the variable set as  $\bar{a}$  ( $a_1 \dots a_p$  represent the phaseshifts,  $a_{p+1}$  is the normalisation) we can then vary  $\chi^2$  with respect to the  $a_j$ . This leads to the set of coupled equations

$$\sum_{s=1}^M (\sigma_x(s) - F(s)) q_j(s) / \delta\sigma_x^2(s) = 0 \quad (2)$$

where

$$q_j(s) = \partial F(s) / \partial a_j. \quad (3)$$

Expanding  $F(s)$  in a Taylor series and substituting (2), we can conveniently write the solution as

$$\bar{B} = \bar{Q} \Delta \bar{a} \quad (4)$$

where

$$B_j = \sum_{s=1}^M (\sigma_x(s) - F^0(s)) q_j(s) / \delta\sigma_x^2(s)$$

$$Q_{j,k} = \sum_{s=1}^M q_j(s) q_k(s) / \delta\sigma_x^2(s)$$

and  $\Delta a_j$  are the first-order Taylor series corrections to the  $a_j$ .

Inverting the real symmetric matrix  $Q$  then allows a simple solution for the  $\Delta a_j$  corrections:

$$\bar{\varepsilon} \bar{B} = \Delta \bar{a} \quad (\bar{\varepsilon} = \bar{Q}^{-1}). \quad (5)$$

The solution then proceeds by estimating the initial values for the phaseshifts and normalisation followed by iterative corrections until an acceptably converged parameter set is achieved.

It has been pointed out by Sin Fai Lam (1982) that, for heavy elements like Xe, relativistic effects may have to be considered for the scattering process and a relativistic phaseshift analysis may be necessary. In this formalism two phaseshifts are associated with each partial wave ( $\eta_l^+$  and  $\eta_l^-$ ) corresponding to the two spin states of the

continuum electron. At resonance energies the two phaseshifts are different and lead to spin polarisation effects. We have omitted in the present paper the resonance regions (to be discussed in a subsequent paper). At non-resonant energies the two phaseshifts are very nearly equal and a non-relativistic phaseshift analysis appears to be satisfactory.

### 2.3. Normalisation procedure

Since the *LS*-coupled phaseshift formalism is not completely appropriate for xenon, it was decided to fit the angular distributions for large and small angle extrapolation purposes but to normalise the resulting data to an empirically derived value for the integral elastic cross section. The relative data were placed on the absolute scale by normalising the integral elastic cross sections at each impact energy to a value obtained semi-empirically from the relationship  $Q_{\text{EL}} = Q_{\text{TOT}} - Q_{\text{ION}} - Q_{\text{EXC}}$ , where the symbols on the right-hand side refer to the total electron scattering, total ionisation and total excitation cross section respectively. Total scattering cross sections available in the 1–100 eV impact energy region are shown in figure 1. We used the values reported by

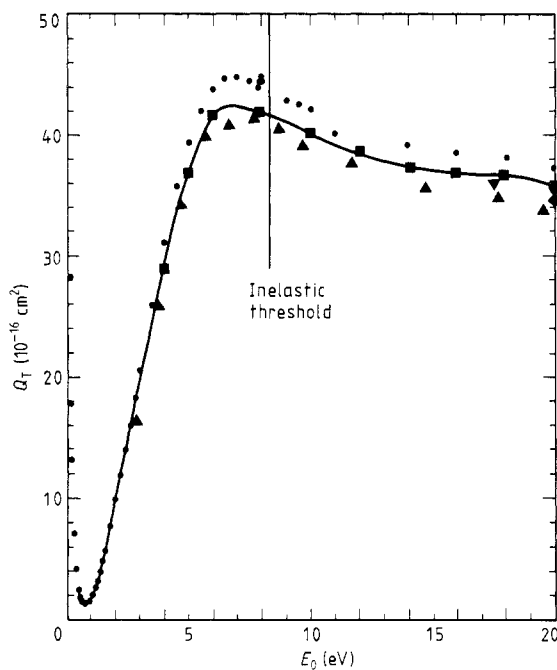


**Figure 1.** Total electron collision cross sections for Xe: ▲, Dababneh *et al* (1980); ◆, Dababneh *et al* (1982); ▼, Wagenaar (1984); ■, Nickel *et al* (1985); and ●, Holtkamp and Jost (1985). The full curve represents the cross sections accepted for the normalisation of the present results.

Nickel *et al* (1985) and extrapolated to low energies on the basis of the results of Jost *et al* (1985). The values of  $Q_{\text{ION}}$  were taken from de Heer *et al* (1979) who made recommendations for these cross sections based on all available ionisation information. De Heer *et al* (1979) also recommended total excitation cross sections. We, however,

used the more recently recommended values given by Hayashi (1983). All these cross sections as well as the deduced  $Q_{\text{EL}}$  values are listed in table 1. The errors associated with the integral elastic cross sections were obtained by taking the square root of the sum of the squares of the per cent errors associated with  $Q_{\text{TOT}}$ ,  $Q_{\text{ION}}$  and  $Q_{\text{EXC}}$ . In each case the per cent error was multiplied by the ratio of the corresponding cross section to the total electron scattering cross section. The unweighted errors were taken as  $\pm 3$ ,  $\pm 5$  and  $\pm 25\%$ , respectively.

**Table 1.** Summary of the total electron scattering, ionisation and excitation cross sections and the integral elastic scattering cross sections derived from them (in units of  $10^{-16} \text{ cm}^2$ ).

$E_0$ (eV)	$Q_{\text{T}}$	$Q_{\text{ION}}^{\text{c}}$	$Q_{\text{EXC}}^{\text{d}}$	$Q_{\text{EL}}^{\text{e}}$
1.00	1.65 <sup>a</sup>	—	—	$1.65 \pm 0.08$
1.75	7.30 <sup>a</sup>	—	—	$7.30 \pm 0.37$
2.75	16.5 <sup>a</sup>	—	—	$16.5 \pm 0.83$
3.75	26.0 <sup>a</sup>	—	—	$26.0 \pm 1.30$
4.75	35.3 <sup>b</sup>	—	—	$35.3 \pm 1.1$
5.75	40.7 <sup>b</sup>	—	—	$40.7 \pm 1.2$
9.75	40.4 <sup>b</sup>	—	—	$40.4 \pm 1.2$
14.75	37.2 <sup>b</sup>	—	—	$37.2 \pm 1.1$
19.75	35.60 <sup>b</sup>	2.30	3.7	$29.60 \pm 1.17$
29.75	21.00 <sup>b</sup>	3.90	3.6	$13.50 \pm 0.72$
49.75	15.80 <sup>b</sup>	4.51	2.4	$8.89 \pm 0.45$
59.75	13.20 <sup>b</sup>	4.50	2.1	$6.60 \pm 0.35$
63.00	13.00 <sup>b</sup>	4.51	2.0	$6.49 \pm 0.34$
80.00	12.40 <sup>b</sup>	4.53	1.66	$6.21 \pm 0.30$
100.00	11.90 <sup>b</sup>	4.70	1.38	$5.82 \pm 0.36$

<sup>a</sup> From Jost *et al* (1984, 1985).

<sup>b</sup> From Nickel *et al* (1985).

<sup>c</sup> From de Heer *et al* (1979).

<sup>d</sup> Hayashi (1983).

<sup>e</sup> Values used for normalising the present cross sections.

### 3. Results and discussion

#### 3.1. Differential cross sections

The phaseshifts obtained by fitting to the measured angular distributions are listed in table 2 and the normalised differential cross sections in table 3. The estimated uncertainties in the DCS are listed as the last entry in each column of table 3. These values were obtained by combining the uncertainty associated with the phaseshift fit and the estimated normalisation and systematic errors.

Following Bevington, we can define the uncertainty for any of the fitted parameters in the phaseshift analysis as

$$\delta a_j^2 = \sum_{s=1}^M \delta \sigma_x^2(s) (\partial a_j / \partial \sigma_x(s))^2 \quad (6)$$

where  $\partial a_j / \partial \sigma_x(s)$  represents the effect of each data point in determining the  $a_j$ . Manipulating terms in the  $\bar{\epsilon}$  matrix (Bevington 1969, ch 8 and 11), it can be shown that

$$\delta a_j^2 = \epsilon_{j,j} \quad (\chi^2 = 1). \quad (7)$$

**Table 2.** Summary of phaseshifts (deg).

$L$ $E_0$ (eV)	0	1	2	3	4	5	6	7
1.00	172.4	181.7	5.57	—	—	—	—	—
1.75	162.3	175.0	9.80	—	—	—	—	—
2.75	145.6	165.8	21.9	—	—	—	—	—
3.75	136.8	160.0	34.3	4.91	—	—	—	—
4.75	136.2	152.0	52.7	8.64	4.44	—	—	—
5.75	121.9	148.6	62.8	11.94	6.26	1.29	—	—
9.75	101.7	120.2	75.2	23.92	5.79	5.13	—	—
14.75	69.7	100.0	72.8	39.9	9.92	5.19	—	—
19.75	52.0	74.2	61.1	53.7	10.3	5.19	1.78	—
29.75	69.6	72.6	56.2	100.7	12.31	7.09	15.76	3.94
49.75	7.95	32.2	43.5	181.0	28.1	12.5	10.5	5.15
59.75	0.998	23.7	30.5	4.62	26.95	14.12	—	—
63.00	1.03	22.0	30.0	6.13	28.1	14.2	—	—
80.00	-3.22	24.0	26.2	14.9	39.1	21.7	—	—
100.00	129.2	13.9	24.1	23.5	52.3	27.3	15.6	13.4

**Table 3.** Elastic differential scattering cross sections ( $10^{-16} \text{ cm}^2 \text{ sr}^{-1}$ ).

$E_0$ (eV) $\theta$ (deg)	1	1.75	2.75	3.75	4.75	5.75	9.75	14.75
15	—	—	—	6.388	12.74	18.77	22.43	34.76
20	0.395	0.422	1.773	5.107	10.33	15.16	22.54	26.77
25	—	0.197	1.231	3.701	7.87	11.13	17.39	19.44
30	0.150	0.0897	0.881	2.731	5.91	8.69	13.67	13.5
32	—	0.0739	—	—	—	—	—	—
35	—	0.0814	0.755	2.147	4.57	6.68	9.92	8.81
40	0.028	0.219	0.812	1.799	3.40	5.32	7.32	5.64
45	0.015	0.399	0.970	1.726	2.85	4.00	5.16	3.33
50	0.033	0.547	1.223	1.813	2.54	3.46	3.81	1.96
55	—	0.736	1.535	2.083	2.47	2.77	2.64	1.22
60	0.098	0.918	1.807	2.317	2.51	2.48	1.96	0.862
65	—	1.064	1.979	2.508	2.61	2.36	1.44	0.705
70	0.160	1.082	2.154	2.692	2.67	2.37	1.18	0.656
75	0.195	1.180	2.131	2.702	2.73	2.27	0.988	0.609
80	0.213	1.104	2.107	2.589	2.66	2.20	0.896	0.556
85	—	1.069	1.915	2.420	2.47	1.99	0.806	0.481
90	0.213	0.942	1.717	2.076	2.14	1.71	0.747	0.429
95	—	0.825	1.356	1.692	1.78	1.33	0.672	0.382
98	—	—	—	—	—	1.07	—	0.366
100	0.198	0.626	1.084	1.253	1.31	0.909	0.601	0.380
102	—	—	—	—	—	—	—	0.381
105	—	0.451	0.706	0.839	0.839	0.560	0.515	0.399
108	—	—	—	—	—	0.351	—	0.436
109	—	—	—	0.529	—	—	—	—
110	0.130	0.303	0.448	0.477	0.454	0.261	0.472	0.461
111	—	—	—	0.384	—	—	—	—
112	—	—	—	0.322	—	0.176	0.441	—
113	—	—	0.283	0.260	—	0.124	—	—
114	—	—	—	—	0.213	0.104	0.440	0.501
115	—	0.192	0.211	0.169	0.150	0.0853	0.434	0.508

Table 3. (continued)

$E_0$ (eV) $\theta$ (deg)	1	1.75	2.75	3.75	4.75	5.75	9.75	14.75
116	—	—	—	—	0.116	0.0677	0.433	—
117	—	—	—	0.099	0.074	0.0504	—	—
118	—	0.115	0.122	0.065	0.0497	0.0488	0.446	—
119	—	—	0.095	0.055	0.035	—	—	—
120	0.062	0.082	0.074	0.034	0.0234	0.0505	0.467	0.556
121	—	—	0.049	0.032	0.0212	—	0.475	—
122	—	0.061	0.047	0.034	0.0243	0.0893	—	—
123	—	—	0.046	—	0.0446	—	0.511	—
124	—	0.055	—	0.059	0.0648	0.162	—	—
125	—	—	0.048	0.077	0.098	0.205	0.556	0.563
126	—	0.037	—	0.119	—	0.271	0.577	—
127	—	—	0.077	—	0.190	—	—	—
128	—	0.032	0.109	0.204	—	—	—	—
129	—	—	—	0.331	—	—	—	—
130	0.030	0.040	0.145	0.322	0.385	0.549	0.710	0.549
132	—	0.047	0.215	—	—	—	—	—
133	—	—	—	0.572	—	—	—	—
134	—	0.062	—	—	0.795	—	0.889	—
135	—	—	0.372	0.717	0.898	1.02	0.924	0.489
136	—	0.074	—	0.861	—	—	—	—
137	—	—	—	—	1.218	—	—	—
138	—	0.097	—	—	—	—	1.066	—
139	—	—	—	—	—	—	—	0.407
140	—	0.117	0.659	1.251	1.63	1.63	1.165	0.382
141	—	—	—	—	—	—	—	0.374
142	—	0.183	—	1.538	—	—	—	0.338
143	—	—	—	—	—	—	—	0.287
144	—	—	—	—	—	—	—	0.250
Error (%)	15	9	7	9	5	8	5	5

$E_0$ (eV) $\theta$ (deg)	19.75	29.75	49.75	59.75	63.0	80.0	100.0
10	—	—	19.60	17.0	17.3	16.8	15.8
14	—	—	—	—	—	—	6.42
15	32.3	13.7	9.48	7.02	6.73	6.76	—
19	—	—	—	—	—	—	1.85
20	23.9	9.08	4.01	2.43	2.33	2.12	—
21	—	—	—	—	—	—	1.28
24	—	—	—	—	—	0.357	—
25	17.3	5.77	1.51	0.684	0.619	0.460	—
26	—	—	—	—	—	—	0.196
27	—	—	—	—	—	0.203	0.154
28	—	—	—	—	—	0.117	0.105
29	—	—	—	—	—	0.081	0.102
30	10.5	3.38	0.503	0.140	0.099	0.053	0.107
31	—	—	—	—	—	0.050	—
32	—	—	—	0.057	0.054	0.056	0.159
33	—	—	—	—	—	0.078	—
34	—	—	—	0.045	0.044	0.096	0.250
35	6.59	1.89	0.176	0.039	0.045	0.118	—
36	—	—	—	—	—	0.144	0.331

**Table 3.** (continued)

$E_0$ (eV) $\theta$ (deg)	19.75	29.75	49.75	59.75	63.0	80.0	100.0
37	—	—	—	0.049	—	—	—
38	—	—	—	—	0.059	—	—
39	—	—	—	—	—	—	0.409
40	3.13	0.890	0.060	0.066	0.085	0.243	—
41	—	—	—	—	—	—	0.420
44	—	—	—	—	—	—	0.412
45	1.25	0.371	0.0241	0.079	0.110	0.298	—
47	—	—	—	—	—	0.292	—
48	0.595	0.206	0.0123	—	—	—	—
49	—	—	—	—	—	—	0.354
50	0.388	0.152	0.0071	0.060	0.092	0.253	—
51	—	—	—	—	—	—	0.313
52	0.230	0.133	0.0047	—	—	—	—
53	0.187	0.132	—	—	—	—	—
54	0.168	0.137	0.0051	—	—	—	0.213
55	0.160	—	—	0.037	0.064	0.171	—
56	0.16	0.163	0.0062	—	—	—	0.173
57	0.175	—	—	—	—	—	—
58	0.207	0.195	0.0090	—	—	—	—
59	—	—	—	—	—	—	0.095
60	0.273	0.239	0.015	0.019	0.027	0.076	0.076
62	0.364	—	—	0.014	0.017	—	0.047
63	—	—	—	0.0096	—	—	—
64	0.453	—	—	—	0.010	—	0.021
65	0.494	0.330	0.031	—	0.0071	0.022	0.015
66	0.536	—	—	0.0074	0.0059	—	—
67	0.566	—	—	—	—	0.011	0.0093
68	0.596	—	—	—	0.0054	0.0093	0.0099
69	—	—	—	0.0077	—	0.0077	0.016
70	0.634	0.371	0.044	0.0080	0.0057	0.0086	—
71	—	—	—	—	—	0.011	0.029
72	—	—	—	0.0086	0.0059	0.012	—
73	—	—	—	—	—	0.016	—
74	—	—	—	—	0.0061	—	0.058
75	0.665	0.350	0.045	0.0099	—	0.023	—
76	—	—	—	—	0.0069	—	0.079
78	—	—	—	0.0096	0.0077	—	—
80	0.591	0.278	0.037	0.0074	0.0064	0.046	0.125
82	—	—	—	0.0056	0.0055	—	—
84	—	—	—	0.0023	0.0044	—	0.152
85	0.453	0.198	0.032	—	—	0.060	—
86	—	—	—	0.0011	0.0032	—	0.161
88	—	—	—	0.0021	0.0025	—	—
90	0.267	0.133	0.041	0.0038	0.0044	0.059	0.157
92	—	—	—	—	0.0074	—	—
93	—	0.116	—	—	—	—	—
94	0.162	—	—	—	—	—	0.136
95	0.141	0.112	0.075	0.026	0.022	0.051	—
96	—	—	—	—	—	—	0.124
97	0.108	0.120	—	—	—	—	—
98	0.089	—	—	—	—	—	—
99	0.081	0.133	—	—	—	—	0.103
100	0.070	—	0.150	0.079	0.055	0.051	—

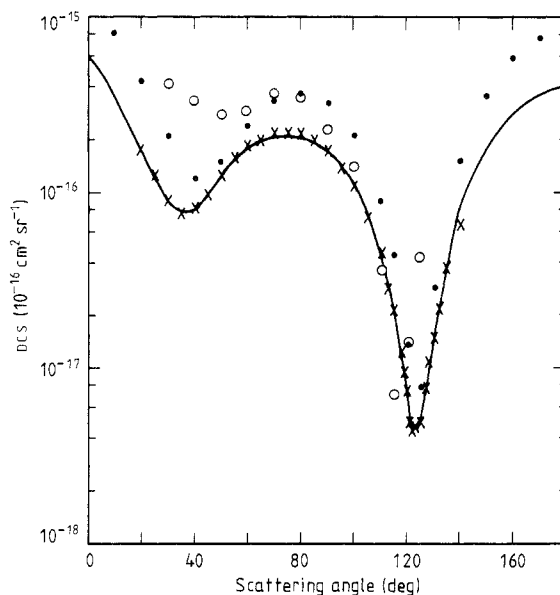


Table 3. (continued)

$\theta$ (deg) \ $E_0$ (eV)	19.75	29.75	49.75	59.75	63.0	80.0	100.0
101	0.063	0.157	—	—	—	—	0.086
102	0.058	—	—	—	—	—	—
103	0.060	0.180	—	—	—	—	—
104	0.062	—	—	—	—	—	0.065
105	0.067	0.212	0.256	0.152	0.113	0.066	—
106	0.071	—	—	—	—	—	0.059
107	0.076	—	—	—	—	—	—
108	0.085	—	—	—	—	—	—
110	0.105	0.297	0.352	0.217	0.161	0.093	0.047
112	—	—	—	—	—	—	0.043
114	—	—	—	—	—	—	0.045
115	0.161	0.339	0.423	0.284	0.238	0.137	—
116	—	—	—	—	—	—	0.056
120	0.196	0.332	0.445	0.314	0.270	0.169	0.065
124	—	—	—	—	—	—	0.074
125	0.199	0.269	0.402	0.297	0.244	0.174	—
129	—	—	—	—	—	—	0.066
130	0.172	0.173	0.315	0.216	0.203	0.140	—
132	—	—	—	—	—	—	0.052
133	—	0.112	—	—	—	—	—
134	—	—	—	—	—	—	0.041
135	0.117	0.074	0.190	0.135	0.125	0.092	—
136	—	0.059	—	—	—	—	0.030
137	—	0.043	—	—	—	—	—
138	—	0.033	—	0.066	0.068	—	0.016
139	—	0.025	—	—	—	—	—
140	0.087	0.018	0.070	0.039	0.033	0.036	0.0074
141	—	0.018	0.053	—	—	0.029	0.0037
142	—	0.021	0.035	0.019	0.015	0.021	0.0017
143	—	0.027	0.025	—	—	0.016	0.0018
144	—	0.037	0.014	0.0022	0.0059	0.014	0.0024
145	—	—	0.0054	—	—	0.0099	0.0060
146	—	—	—	—	—	0.0076	0.0098
Error (%)	6	9	7	7	7	9	13

In order to arrive at the  $\chi^2 = 1$  condition, the  $\chi^2$  of the final fit is calculated and then used to scale the  $\delta\sigma_x(s)$  appropriately. The interpretation of this procedure is that changing any of the  $a_j$  separately by an amount  $\Delta a_j$  will result in a  $\Delta\chi^2$  of 1. Using this procedure, estimated errors in the phaseshifts and the fitted normalisation parameter can be obtained. The latter value, which is quite sensitive to small and large angle data points, is taken as the estimated uncertainty in the fit. The uncertainties related to the integral elastic cross sections are taken as listed in table 1. Due to the care exercised in the experimental arrangement and background correction, the errors from systematic causes are estimated to be no larger than 3%. The square roots of the sum of the squares of all these errors yield the overall errors given in table 3.

At impact energies which are less than the inelastic threshold our results at 2.75 and 4.75 eV can be compared with the recent results of Nishimura *et al* (1985) at 3 eV and Holtkamp and Jost (1985) at 5 eV, respectively. Substantial deviation is present



**Figure 2.** Differential scattering cross sections:  $\times$ , present results, 2.75 eV;  $\circ$ , Nishimura *et al* (1983), 3 eV;  $\bullet$ , McEachran and Stauffer (1984), 2.75 eV. The full curve is the phaseshift fit.

between the two experimental results at 2.75 eV (figure 2) which may partly be due to the different impact energy. The phaseshift fit to the present data points is indicated by the full curves in figure 2. The theoretical cross sections obtained by McEachran and Stauffer at 2.75 eV are also shown and agree quite well with the present data in shape but differ in magnitude by about a factor of two. The 4.75 and 5 eV cross sections are in good agreement except in the region of the deep minimum at around  $120^\circ$  scattering angle. At 1.0 and 1.75 eV, we have no DCS available with which the present results could be compared (although Weyhreter *et al* (1983) have reported some results in the 50 meV–2 eV impact energy range at a conference). The DCS available from Klewer *et al* (1980) at 2, 5.5 and 7.5 eV and from Heindorf *et al* (1976) at 3, 5 and 7.5 eV impact energies differ significantly in shape from the present DCS curves at nearby energies.

More extensive data (both experimental and theoretical) are available at impact energies above the inelastic threshold. Comparisons of our results at 14.75, 19.75, 59.75 and 100.0 eV are made with other recent data. Reasonably good agreement is found between the present 14.75 eV cross sections and those of Nishimura *et al* (1985) at 15 eV. The various 20 eV results (figure 3) show good agreement in shape with the present 19.75 eV DCS curves, but substantial differences exist in magnitude among them and the theoretical results are again about a factor of two larger than the present ones. At 59.75 (60.0) and 100 eV we find good agreement among the present results and those of Holtkamp and Jost (1985) and Nishimura *et al* (1985). The 59.75 (60.0) eV results are shown in figure 4. The earlier cross sections of Williams and Crowe (1975) differ substantially from our results at 20, 60 and 100 eV impact energies at certain angles (not shown in our figures). At 100 eV the DCS available from Jansen and de Heer (1976) in the  $5$  to  $50^\circ$  angular range (not shown) are in good agreement with the present data.

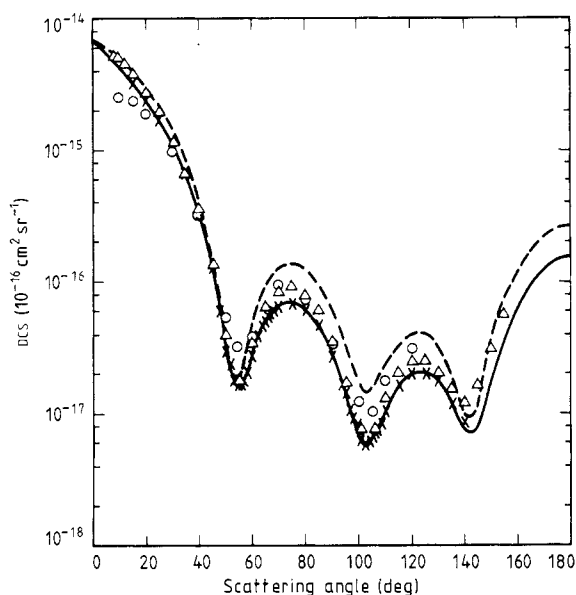


**Figure 3.** As figure 2 except that the present results shown are at 19.75 eV and those of Nishimura *et al* at 20 eV. In addition:  $\Delta$ , Holtkamp and Jost (1985), 20 eV; ---, McEachran and Stauffer (1984), 20 eV.

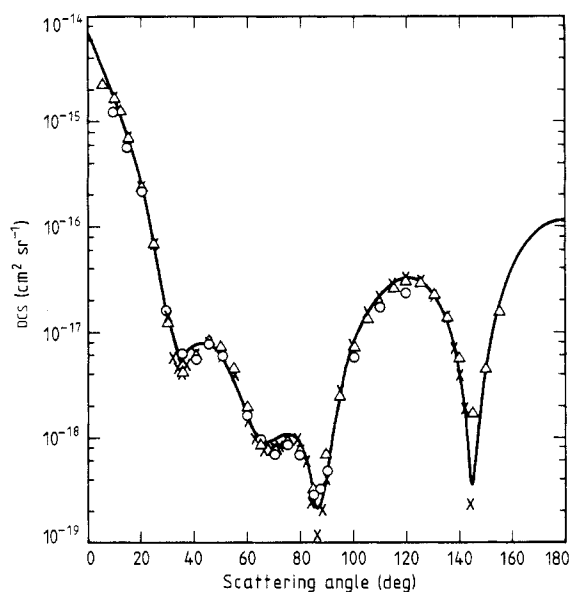


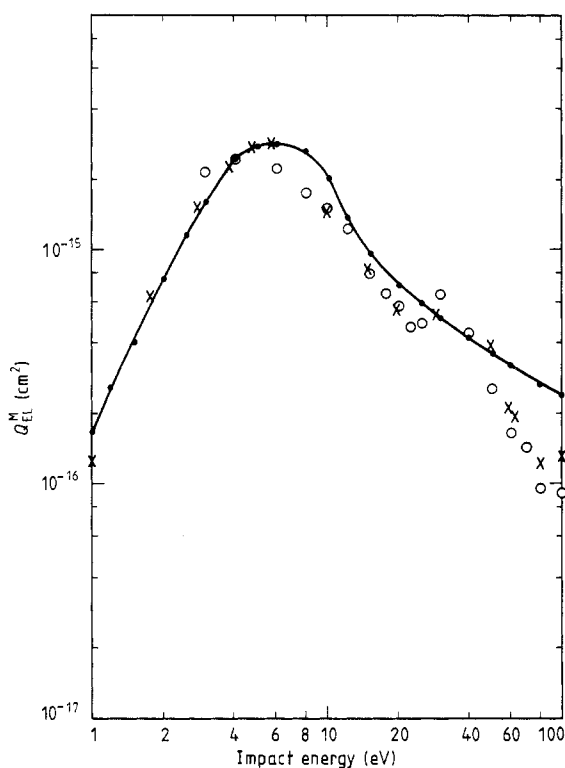
**Figure 4.** As figure 2 except that the present results shown are at 59.75 eV, those of Nishimura *et al* at 60 eV and no data from McEachran and Stauffer. In addition:  $\Delta$ , Holtkamp and Jost (1985), 60 eV.

### 3.2. Momentum transfer cross sections

The momentum transfer cross sections calculated from the DCS are given in table 4 and figure 5 and are compared with the results of Nishimura *et al* (1985) and with the recommended values given by Hayashi (1983) based on all available information a

**Table 4.** Momentum transfer cross sections ( $10^{-16}$  cm<sup>2</sup>).

$E_0$ (eV)	$Q_{\text{EL}}^{\text{M}}$		$E_0$ (eV)	$Q_{\text{EL}}^{\text{M}}$	
	Present	Hayashi <sup>a</sup>		Present	Hayashi <sup>a</sup>
1.00	1.24	1.7	19.75	5.44	7.2
1.75	6.32	5.8	29.75	5.33	5.1
2.75	15.20	13.9	49.75	3.95	3.6
3.75	23.19	22.5	59.75	2.12	3.2
4.75	27.37	27.5	63.00	1.92	3.1
5.75	28.04	28.5	80.00	1.24	2.7
9.75	14.62	21.0	100.00	1.36	2.4
14.75	8.33	9.8			

<sup>a</sup> Obtained by interpolation from the curve in figure 5.**Figure 5.** Momentum transfer cross sections: x, present results; O, Nishimura *et al* (1985); —●—, Hayashi (1983).

that time. The agreement between the experimental data is good considering the arbitrariness in extrapolating the differential cross sections to 180°. The values recommended by Hayashi seem to be too large at around 8 eV and above 60 eV impact energies.

## Acknowledgments

We would like to express our gratitude to A Danjo, G Holtkamp, K Jost, T Matsuda and H Nishimura for supplying us with their data prior to publication and to M Hayashi and L T Sin Fai Lam for valuable discussions. The research described in this paper was performed at the Jet Propulsion Laboratory, California Institute of Technology and was sponsored by the National Aeronautics and Space Administration.

## References

- Berg H P 1982 *Phys. Lett.* **88A** 292  
Bevington P R 1969 *Data Reduction and Error Analysis for the Physical Sciences* (New York: McGraw Hill)  
Brandsen B H and McDowell M R C 1978 *Phys. Rep.* **46** 249  
Brinkmann R T and Trajmar S 1981 *J. Phys. E: Sci. Instrum.* **14** 425  
Dababneh M S, Kauppila W E, Downing J P, Laperrier F, Pol V, Smart J H and Stein T S 1980 *Phys. Rev. A* **22** 1872-7  
Dababneh M S, Hsieh Y F, Kauppila W E, Pol V and Stein T S 1982 *Phys. Rev. A* **26** 1252-9  
Hall R T, Chutjian A and Trajmar S 1973 *J. Phys. B: At. Mol. Phys.* **6** L365  
Hayashi M 1983 *J. Phys. D: Appl. Phys.* **16** 581-9  
de Heer F J, Jansen R H J and van der Kaay W 1979 *J. Phys. B: At. Mol. Phys.* **12** 979  
Heindorff T, Hoff T and Dabkiewicz P 1976 *J. Phys. B: At. Mol. Phys.* **9** 89-99  
Holtkamp G and Jost K 1985 Private communication  
Jansen R H J and de Heer F J 1976 *J. Phys. B: At. Mol. Phys.* **9** 213-26  
Jost K, Bisling P G F, Eschen F, Feismann M and Walther L 1983 *Proc. 13th Int. Conf. on the Physics of Electronic and Atomic Collisions (Berlin) 1983* ed J Eichler, W Fritsch, I V Hertel, N Stolterfoht and U Wille (Amsterdam: North-Holland) Abstracts p 91  
— 1985 Private communication  
Kemper K, Awe B, Rosicky F and Feder R 1985 *J. Phys. B: At. Mol. Phys.* **16** 1819  
Klewer M, Beerlage M J M and van der Wiel M J 1980 *J. Phys. B: At. Mol. Phys.* **13** 571-86  
McEachran R P and Stauffer A D 1984 *J. Phys. B: At. Mol. Phys.* **17** 2507-18  
Nickel J C, Imre K, Register D F and Trajmar S 1985 *J. Phys. B: At. Mol. Phys.* **18** 125-33  
Nishimura H, Danjo A and Matsuda T 1985a *Proc. 14th Int. Conf. on the Physics of Electronic and Atomic Collisions (Palo Alto) 1985* ed M J Coggiola, D L Huestis and R P Saxon (Amsterdam: North-Holland) Abstracts p 108  
— 1985b Private communication  
O'Connell J K and Lane N F 1983 *Phys. Rev. A* **27** 1983  
Register D F, Trajmar S and Srivastava S K 1980 *Phys. Rev. A* **21** 1134  
Sin Fai Lam L T 1982a *J. Phys. B: At. Mol. Phys.* **15** 119  
— 1982b Private communication  
Srivastava S K, Chutjian A and Trajmar S 1975 *J. Chem. Phys.* **63** 2659  
Wagenaar R 1984 *Thesis* Amsterdam  
Williams J F and Crowe A 1975 *J. Phys. B: At. Mol. Phys.* **8** 2233-48  
Weyhreter M, Barzick B and Linder F 1983 *Proc. 13th Int. Conf. on the Physics of Electronic and Atomic Collisions (Berlin) 1983* ed J Eichler, W Fritsch, I V Hertel, N Stolterfoht and U Wille (Amsterdam: North-Holland) p 78